LIMNOLOGY
and
OCEANOGRAPHY: METHODS

Limnol. Oceanogr.: Methods 12, 2014, 264–280

Application and assessment of a membrane-based pCO_2 sensor under field and laboratory conditions

Zong-Pei Jiang[1,2], David J. Hydes[1], Sue E. Hartman[1], Mark C. Hartman[1], Jon M. Campbell[1], Bruce D. Johnson[3], Bryan Schofield[3], Daniela Turk[4,5], Douglas Wallace[4], William J. Burt[4], Helmuth Thomas[4], Cathy Cosca[6], and Richard Feely[6]*

[1]National Oceanography Centre Southampton, European Way, Southampton, UK, SO14 3ZH
[2]Ocean College, Zhejiang University, Hangzhou, China
[3]ProOceanus Systems Inc., Bridgewater, Nova Scotia, Canada
[4]Department of Oceanography, Dalhousie University, Halifax, NS, Canada
[5]Lamont-Doherty Earth Observatory, Columbia University, NY, USA
[6]Pacific Marine Environmental Lab, NOAA, Seattle, WA, USA

Abstract

The principle, application, and assessment of the membrane-based ProOceanus CO_2-Pro sensor for partial pressure of CO_2 (pCO_2) are presented. The performance of the sensor is evaluated extensively under field and laboratory conditions by comparing the sensor outputs with direct measurements from calibrated pCO_2 measuring systems and the thermodynamic carbonate calculation of pCO_2 from discrete samples. Under stable laboratory condition, the sensor agreed with a calibrated water-air equilibrator system at –3.0 ± 4.4 μatm during a 2-month intercomparison experiment. When applied in field deployments, the larger differences between measurements and the calculated pCO_2 references (6.4 ± 12.3 μatm on a ship of opportunity and 8.7 ± 14.1 μatm on a mooring) are related not only to sensor error, but also to the uncertainties of the references and the comparison process, as well as changes in the working environments of the sensor. When corrected against references, the overall uncertainties of the sensor results are largely determined by those of the pCO_2 references (± 2 and ± 8 μatm for direct measurements and calculated pCO_2, respectively). Our study suggests accuracy of the sensor can be affected by temperature fluctuations of the detector optical cell and calibration error. These problems have been addressed in more recent models of the instrument through improving detector temperature control and through using more accurate standard gases. Another interesting result in our laboratory test is the unexpected change in alkalinity which results in significant underestimation in the pCO_2 calculation as compared to the direct measurement (up to 90 μatm).

The knowledge of surface ocean CO_2 variability is important for understanding the marine carbon cycle and its future response to the absorption of anthropogenic CO_2 (Doney et al. 2009). In the past few decades, high-accuracy seawater pCO_2 measuring systems (Körtzinger et al. 1996; Dickson et al. 2007; Pierrot et al. 2009) have been widely used on research vessels providing high quality pCO_2 data, which leads to the generation of a global atlas of the surface ocean pCO_2 (Surface Ocean CO_2 Atlas, http://www.socat.info/, Bakker et al. 2013) and CO_2 flux (Takahashi et al. 2009). However, there is still a lack of data from large areas of the globe, especially in the shelf seas, Southern Ocean, and southern-hemisphere subtropical gyres (Doney et al. 2009). Moreover, changes in seawater pCO_2 can occur on timescales from daily (Degrandpre et al. 1998; Yates et al. 2007; Dai et al. 2009; Turk et al. 2013) to seasonal and interannual (Bates 2002, 2007; Watson et al. 2009; Jiang et al. 2013), especially in the dynamic coastal environments (Borges and Frankignoulle 1999; Thomas and Schneider 1999; De La Paz et al. 2008; Turk et al. 2010; Jiang et al. 2011). Observations with sufficient temporal and spatial resolution are thus needed for a better understanding of the controlling mechanism of pCO_2 variability in different regions and for a more reliable CO_2 flux estimation.

In addition to the traditional shipboard measuring system (e.g., the General Oceanics pCO_2 measuring system), there are emerging techniques to develop autonomous pCO_2 sensors.

*Corresponding author: E-mail: zongpei.jiang@noc.soton.ac.uk

Acknowledgments

Full text appears at the end of the article.

DOI 10.4319/lom.2014.12.264

Table 1. The various designs of pCO_2 sensors.

Equilibrator	Measured phase	Determination	References
Direct contact of water-gas	gas	NDIR	Körtzinger et al. (1996); ACT (2009a); Nemoto et al. (2009)
Gas permeable interface	gas	NDIR	Kayanne et al. (2002); Fiedler et al. (2012); Saderne et al. (2013), this study
Gas permeable interface	indicator solution	electrode	Shitashima 2010
Gas permeable interface	indicator solution	fluorescence	Goyet et al. (1992); Tabacco et al. (1999); Rubin and Ping Wu (2000)
Gas permeable interface	indicator solution	spectrophotometry	Degrandpre (1993); Lefévre et al. (1993); Degrandpre et al. (1995, 1999); Wang et al. (2002); Wang et al. (2003); Nakano et al. (2006); Lu et al. (2008)

As summarized in Table 1, these sensors generally follow the same basic concept based on the measurement of a gas or indicator solution that is in equilibrium with the seawater to be determined. The equilibrium state can be reached by using water-gas equilibrators where the gas is directly in contact with the seawater, or via gas permeable interfaces such as polydimethylsiloxane (PDMS) or polytetrafluoroethene (PTFE) membrane. The equilibrated gas can be measured by a nondispersive infrared (NDIR) spectrometry, while the equilibrated indicator solution can be determined by electrode, fluorescence, or spectrophotometric methods (Table 1). For these reagent-based fiber optic chemical sensors (Goyet et al. 1992; Degrandpre 1993; Lefévre et al. 1993; Degrandpre et al. 1995), improvements have been made by using multi-wavelength detection and long pathlength liquid-core waveguides for better precision and accuracy (Degrandpre et al. 1999; Wang et al. 2002; Wang et al. 2003; Nakano et al. 2006; Lu et al. 2008). Evolving sensor technology has enabled cost-effective pCO_2 measurements to be made on various platforms such as ship of opportunity (SOO), buoy and mooring, glider, profiling float, and autonomous underwater vehicle (Degrandpre et al. 1998; Nakano et al. 2006; Nemoto et al. 2009; Willcox et al. 2009; Fiedler et al. 2012; Saderne et al. 2013).

In this article, we describe the principle and design of a membrane-based NDIR pCO_2 sensor (ProOceanus CO_2-Pro, hereafter referred to as CO_2-Pro). The sensor's functionality, reliability, and accuracy are evaluated under various situations including: a 16-d coastal mooring deployment test adjacent to a coral reef in Hawaii (Oct to Nov 2009), shipboard underway mapping on a SOO (Oct 2009 to Mar 2012), intercomparison with a calibrated water-gas equilibrator system in the Aquatron Laboratory at Dalhousie University (May to Sep 2012) and long-term open-ocean mooring deployment in the Northeast Atlantic (Jun 2010 to Jul 2012). The performance of the CO_2-Pro is assessed by comparing the sensor outputs against two kinds of reference: (1) the thermodynamic carbonate calculation of pCO_2 from the determinations of dissolved inorganic carbon (DIC), total alkalinity (TA), and pH from discrete samples; (2) direct measurements by the traditional water-gas equilibrator NDIR systems, which are regularly calibrated against standard gases. The advantages and limitations of the CO_2-Pro are summarized, and the recent improvements of the instrument are introduced.

Materials and procedures

Principle of the CO_2-Pro

The CO_2-Pro is designed as a lightweight, compact, plug and play, versatile instrument for pCO_2 measurements on moorings, drifters, and profilers, in underway mode and in laboratories. As shown in Fig. 1, the sensor is fitted with an equilibrator composed of a gas permeable PDMS membrane (other membrane materials are also available) and an internal detection loop with a NDIR detector based on a highly modified PPSystems SBA-4 CO_2 analyzer. The patented gas transfer interface of the equilibrator features a tubular design, through which the equilibration between the surrounding water and the internal gas stream can be achieved. Copper wire is wound round the tube to inhibit the potential for bio-film formation and the equilibrator is protected from physical damage by an end-cap. An associated Seabird Electronics SBE 5M submersible pump flows water past the outer surface of the equilibrator membrane to accelerate the equilibration. The response time, i.e., the time for the membrane to reduce the perturbation in pCO_2 by a factor of 1/e, is typically 2 min depending on the pumping rate. NDIR measurement on the equilibrated internal gas is taken at a wavelength of 4.26 μm at a controlled optical cell temperature (30°C, 40°C, or 55°C). In addition, temperature, pressure, and humidity of the internal gas are determined to correct the CO_2 measurement. Further detailed specifications of the CO_2-Pro can be found at the company's website http://www.pro-oceanus.com/co2-pro.php.

When the sensor is turned on, the optical cell of the detector warms up and then stabilizes at the temperature set point. A zero point calibration (ZPC) is then carried out to provide a zero-CO_2 baseline (C_{zero}) for the subsequent NDIR absorption measurement. This is done by circulating the internal gas through a CO_2 absorption chamber containing soda lime or Ascarite (flow path: valve 2–circulation pump–optical cell–valve 3–absorption chamber–valve 2, Fig. 1). When the ZPC finishes, the solenoid valves 2 and 3 are activated to cir-

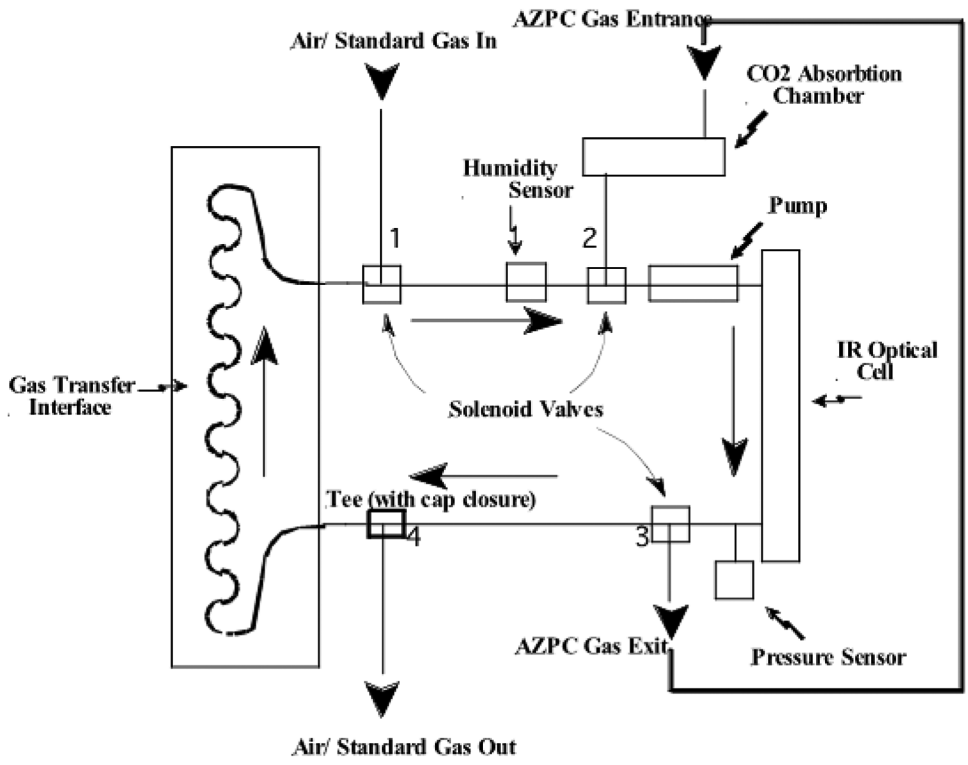

Fig. 1. Schematic of the flow paths of the ProOceanus CO_2-Pro™ pCO_2 sensor. See the text for details.

culate the internal gas around a closed circuit connecting the equilibrator and detector (flow path: valve 2–circulation pump–optical cell–valve 3–valve 4–equilibrator–valve 1–valve 2, Fig. 1). The inferred signal of the internal gas (C_{meas}) is measured to calculate the absorbance ($\varepsilon = C_{meas}/ C_{zero}$) and CO_2 concentration. Once the internal gas is fully equilibrated with the water surrounding the equilibrator (typically 10-15 min after the ZPC), the seawater CO_2 concentration can be determined. The CO_2-Pro features a programmable regular automatic ZPC function to correct the detector drift that can be caused by contamination of the optical cell, optical source aging, and changes in detector sensitivity.

Each CO_2-Pro is factory calibrated at a known optical cell temperature and pressure against 5 standard gasses with xCO_2 (mole fraction of CO_2 in dry air) spanning from 0 to 600 ppm (other calibration ranges are also available). The calibration equation is obtained by a three-segment least-squares fitting to a quadratic equation between ε and xCO_2. This equation is tested subsequently by measuring a further three known mixtures of CO_2. While the calibration equation provides a raw xCO_2 from the inferred measurement, empirical corrections are applied to account for the differences of conditions between calibration and measurement (temperature, pressure, water vapor). As the actual measurement is made on gas which is nearly saturated with water vapor, the output of CO_2-Pro is the mole fraction of CO_2 in wet air (wCO_2, ppm) and pCO_2 in the measured water is obtained by $pCO_2 = wCO_2 \times P_{wet}$, where P_{wet} is the measured total pressure of the internal gas which includes water vapor pressure.

ACT coastal mooring test

The application of the CO_2-Pro in coastal moorings was previously tested in a demonstration project organized by the Alliance for Coastal Technologies (ACT) (http://www.act-us.info/evaluations.php#pco2). During October and November 2009, a CO_2-Pro was mounted on a surface mooring and deployed at a fixed depth of 1 m close to a shallow sub-tropical coral reef in Kaneohe Bay, Hawaii. Continual measurements were made by the CO_2-Pro on an hourly basis, and the results were compared with the reference pCO_2 calculated from discrete samples. pH and TA of these samples were measured spectrophotometrically using meta-cresol purple and bromo-cresol green as indicators, respectively (Dickson et al. 2007). Both measurements were calibrated against the Certified Reference Material (CRM) from Scripps Institution of Oceanography. The accuracy of the pH measurement was estimated to be 0.005 and the standard deviation (SD) of repeated TA measurements was 1.9 μmol kg^{-1} (ACT 2009b). Details of the deployment, measurements, calculation, and quality control were documented by ACT (2009a, 2009b).

SNOMS underway measurements

From June 2007 to March 2012, CO_2-Pro sensors were used for continuous shipboard underway measurement in the operation of a SOO-based measuring system (referred to as SNOMS) on the MV *Pacific Celebes* (Hydes et al. 2013). For

these measurements, a CO_2-Pro was mounted in a 45-liter flow-through pressure tank, together with other sensors for temperature, conductivity, dissolved oxygen, and total dissolved gas pressure. To adapt it to the SNOMS tank, the protecting end-cap and the associated water pump of the CO_2-Pro were removed. The gas transfer interface was thus directly exposed to the seawater for pCO_2 measurement, which also enabled direct cleaning of the membrane surface. The SNOMS tank was fed at a flow rate of 28 ± 2 liters min^{-1} by a branch of the non-contaminated seawater being pumped to the ship's fresh water generator. This water supply was routinely turned off in shallow and potentially turbid water, thereby preventing sedimentation in the tank and contamination of the membrane of the CO_2-Pro. At each port, the tank was opened and the CO_2-Pro membrane was cleaned by hosing it down with fresh water.

The CO_2-Pro was continuously working when the SNOMS system was in operation. The frequency of the automatic ZPC was set to be 6 hours, and the 15 minutes of data after each ZPC (when the internal gas was re-equilibrating with the water) was discarded. In order to account for the difference between the water temperature in the tank (T_{tank}) and that in the surface ocean, an insulated Seabird 48 hull-contact temperature sensor was used to monitor the sea surface temperature (SST). The time lag between SST and T_{tank} was estimated to be ~30 seconds. By considering the temperature effect on pCO_2 (Takahashi et al. 1993), the tank water pCO_2 measured by CO_2-Pro ($pCO_{2,Pro}$) was corrected to the sea surface condition: $pCO_{2,SST} = pCO_{2,Pro} \times \exp[0.0423 \times (SST - T_{tank})]$. The likely accuracy of SST from the hull measurement is 0.1°C (Beggs et al. 2012), which results in an uncertainty of ~1.5 μatm in converting $pCO_{2,Pro}$ to $pCO_{2,SST}$.

In addition to the underway measurements, discrete samples were collected by the ship's engineers for the determination of DIC and TA (Dickson et al, 2007). These samples were shipped to the National Oceanography Centre, Southampton (NOCS) and were measured under stable laboratory conditions. The CRM-calibrated measurements of DIC and TA were carried out using a VINDTA 3C. Repeat measurements on pooled samples were undertaken before sample analysis each day ($n > 3$), these suggested a precision better than ± 2 μmol kg^{-1} for DIC and ± 1.5 μmol kg^{-1} for TA, respectively.

The Aquatron laboratory test

After the operation on the MV *Pacific Celebes*, a controlled test of the CO_2-Pro as a part of the SNOMS tank was carried out in the Aquatron Laboratory at Dalhousie University during May and Sep 2012. To carry out this test, a two cubic meter open tank (referred to as the Aquatron tank) was set up beside the SNOMS tank. The two tanks were filled with sand-bed filtered seawater pumped from an adjacent harbor (estuary) on 23 May. The water was continuously pumped in a circuit between the two tanks with a turnover time of about 2 hours. The pCO_2 of the tank water was monitored by the CO_2-Pro in the SNOMS system, which operated in a similar way as on the MV *Pacific Celebes*. After a stabilization period of ~50 days when the pCO_2 reached a relatively constant range, another pCO_2 measuring system (referred to as the NOIZ system) was set up in the Aquatron tank for a side-by-side comparison with the CO_2-Pro. In order to control pCO_2 to ocean values during the two-month intercomparison exercise (13 Jul to 11 Sep), a simple system was developed to bubble CO_2-free gas (laboratory air passing through a cartridge filled with soda lime) into the Aquatron tank on three occasions (started on 10 Jul, 2 Aug, and 31 Aug, Fig. 6).

The NOIZ system consisted of a bubble type water-gas equilibrator and a Licor 7000 NDIR detector (Körtzinger et al. 1996). The equilibrator was mounted on the Aquatron tank and its lower part was submerged in the water to minimize the temperature difference between the tank water and that in the equilibrator. The detector was calibrated every a few days with zero CO_2 concentration nitrogen gas and an air mixture calibrated with National Oceanic and Atmospheric Administration (NOAA) standard gas before 27 Aug 2012. After that, the calibration directly used a NOAA-supplied standard gas with an uncertainty of ± 1 ppm. No shift could be identified in the calibration when calibration gasses were changed. The accuracy of the pCO_2 measured by the NOIZ system was estimated to be within 2 μatm.

In additional to the pCO_2 measurements, discrete samples for DIC and TA were collected throughout the test on a daily basis. Nutrient samples were collected from 5 Jun onwards for determination of nitrate, silicate, phosphate, and ammonia (Whitledge et al. 1981). To compensate for water loss due to sampling and evaporation, the Aquatron tank was topped up every 4-7 d with newly pumped water. Although this water was pumped from the same location, it may have different properties compared with the original tank water due to the temporal variability at the sampling site. However, these top up events only had a minor influence on the chemical concentrations of the tank water because of the relatively small volumes added (0.2-3% of the total volume of the Aquatron tank). One exception was a substantial top up on 7 Aug (35% of the total volume) because of a large drainage from the sampling tube, which significantly changed the properties of the tank water (see the results section below).

Long-term in situ operation on the PAP mooring

Since June 2010, the CO_2-Pro was used for long-term in situ deployment at the Porcupine Abyssal Plain site (PAP, 49°N 16.5°W, 4800 m water depth), which is the longest running multidisciplinary observatory in the Northeast Atlantic (Hartman et al. 2012). It was deployed on a sensor frame at a fixed depth of 30 m together with other autonomous sensors for temperature, salinity, chlorophyll a fluorescence, and nitrate. All these sensors were controlled by a hub controller, which communicated with NOCS via satellite in near real-time. The CO_2-Pro was powered by the solar panels on the mooring and its measurement frequency and the time length for each measurement could be changed remotely.

Table 2. The estimated uncertainties of the pCO_2 (μatm) calculated from various inputs (pH and TA, or DIC and TA) in this study.

		Sources of uncertainty in pCO_2 calculation				
	Measured pCO_2	pK_1, pK_2	TA	DIC	pH	Uncertainty of the calculated pCO_2
ACT	280 to 840	4 to 12	0.5		6.8	7.5
SNOMS	300 to 500	7 to 10	2.3	3.8		8.1
Aquatron	280 to 860	6 to 15	4.4	6.6		9.9

The carbonate system calculation

The marine carbonate system can be characterized from any two of the four parameters: DIC, TA, pCO_2, and pH (Zeebe and Wolf-Gladrow 2001). In this study, the Excel program "CO2SYS" (Pierrot et al. 2006) was used for the carbonate calculations. The dissociation constants of carbonic acid (pK_1 and pK_2) determined in real seawater by Millero et al. (2006) are in good agreement with previous measurements (Mehrbach et al. 1973; Mojica Prieto and Millero 2002), and are more reliable than those measured in artificial seawater (Millero et al. 2006). Therefore, we chose to use the constants of Millero et al. (2006) in our CO2SYS calculations. The sulphuric dissociation constants were chosen as Dickson (1990) and the total boron fomulation was selected as Lee et al. (2010). In this study, pCO_2 was calculated either from the combination of pH and TA (ACT test) or DIC and TA (SNOMS and Aquatron test). The uncertainty of the pCO_2 calculation comes from inaccuracies in the thermodynamic dissociation constants (mainly pK_1 and pK_2) and the experimental measurements of the variables used for calculation (Millero et al. 2006). As shown in Table 2, the various sources of uncertainties associated with the carbonate calculation yield uncertainties in the calculated pCO_2 which are estimated to be ± 7.5 μatm for the ACT test (ACT 2009a, 2009b), ± 8.1 μatm for the SNOMS operation and ± 9.9 μatm for the Aquatron test within the measured pCO_2 ranges, respectively.

Assessment

Results of the ACT coastal mooring test

The results of the ACT mooring test have been reported by ACT (2009a) and are briefly summarized here. During the 16-d continuous measurement in Kaneohe Bay, nearly 100% of the data were retrieved except for the data gaps during calibration cycles. The hourly time series data from the CO_2-Pro ($pCO_{2,Pro}$ in Fig. 2A, 280-840 μatm) shows a significantly greater dynamic range compared with the values calculated from pH and TA ($pCO_{2,pHTA}$, 314-608 μatm). The higher measurement frequency of the CO_2-Pro thus better characterized the short-term variability of pCO_2 that was mainly caused by the strong biological activities of the adjacent coral reef system.

The 5-min averages of the sensor outputs bracketing the time of discrete sample collection were compared with the calculated $pCO_{2,pHTA}$ in Fig. 2. The mean and SD of the differences between the paired $pCO_{2,Pro}$ and $pCO_{2,pHTA}$ measurements (δpCO_2 = $pCO_{2,Pro}$ - $pCO_{2,pHTA}$, Fig. 2C, δpCO_2 refers to the difference between the raw/corrected sensor output and the pCO_2 reference, the same hereafter) are 8.7 ± 14.1 μatm. $pCO_{2,Pro}$ shows a tight correlation with $pCO_{2,pHTA}$ (R^2 = 0.99, n = 29, not shown), and the positive correlation between δpCO_2 and $pCO_{2,Pro}$ suggests an increasing offset under high pCO_2 conditions (Fig. 2B). This indicates that the δpCO_2 may have been subject to a linear calibration error. When $pCO_{2,Pro}$ is corrected against $pCO_{2,pHTA}$, the SD of the difference between the corrected sensor output ($pCO_{2,ProCorr}$) and $pCO_{2,pHTA}$ is ± 7.4 μatm ($\delta pCO_{2,corr}$ in Fig. 2D), which is similar to the uncertainty of $pCO_{2,pHTA}$ calculation (± 7.5 μatm). There are no systematic changes in $\delta pCO_{2,corr}$ (Fig. 2D), which suggests no other significant sources of error (i.e. biofouling, instrument drift) during the measurement. While the CO_2-Pro performed well among submersible CO_2 sensors in the study (ACT 2009a), the potential error in sensor measurement resulting from temperature fluctuation of the optical cell (see the PAP result section below) was not considered in the performance report by ACT (2009a).

Results of the SNOMS underway measurement

The CO_2-Pro units used in the SNOMS operation were factory calibrated on a yearly basis. For evaluation purposes, $pCO_{2,Pro}$ is compared with the $pCO_{2,DICTA}$ calculated from the daily DIC and TA samples, as well as to direct measurements from other pCO_2 measuring systems in the same region. As the pCO_2 measurements were intermittent at the beginning of the SNOMS project during the circumnavigation of the MV *Pacific Celebes* (2007-2009), the assessment presented below is based on the continuous measurements along the repeated transects in the Pacific (2009 onwards). From Oct 2009 to Feb 2012, the cargo ship in total made 18 transects between the western US coast, New Zealand, and Australia and two CO_2-Pro units were used for measurement in turn (Table 3). Of the 14 transects with successful instrumental measurements (other 2 transects failed with sensor malfunction), there are 12 transects with DIC and TA data.

The difference between the raw sensor output $pCO_{2,Pro}$ (5-min average corresponding to the sampling time) and $pCO_{2,DICTA}$ is shown in Fig. 3A. The overall offset (δpCO_2 = $pCO_{2,Pro}$ - $pCO_{2,DICTA}$) for the 12 transects is 6.4 ± 12.3 μatm (n = 200). No correlation between δpCO_2 and the absolute concentration of pCO_2 (300–500 μatm) is identified (not shown). It is noted that the mean and SD of δpCO_2 vary from transect to transect (Table 3). Aside from any error and potential drift of the sensor, the difference in δpCO_2 among transects may be caused by several other factors: 1) uncertainty in the $pCO_{2,DICTA}$ calculation; 2) the different responses of the two CO_2-Pro

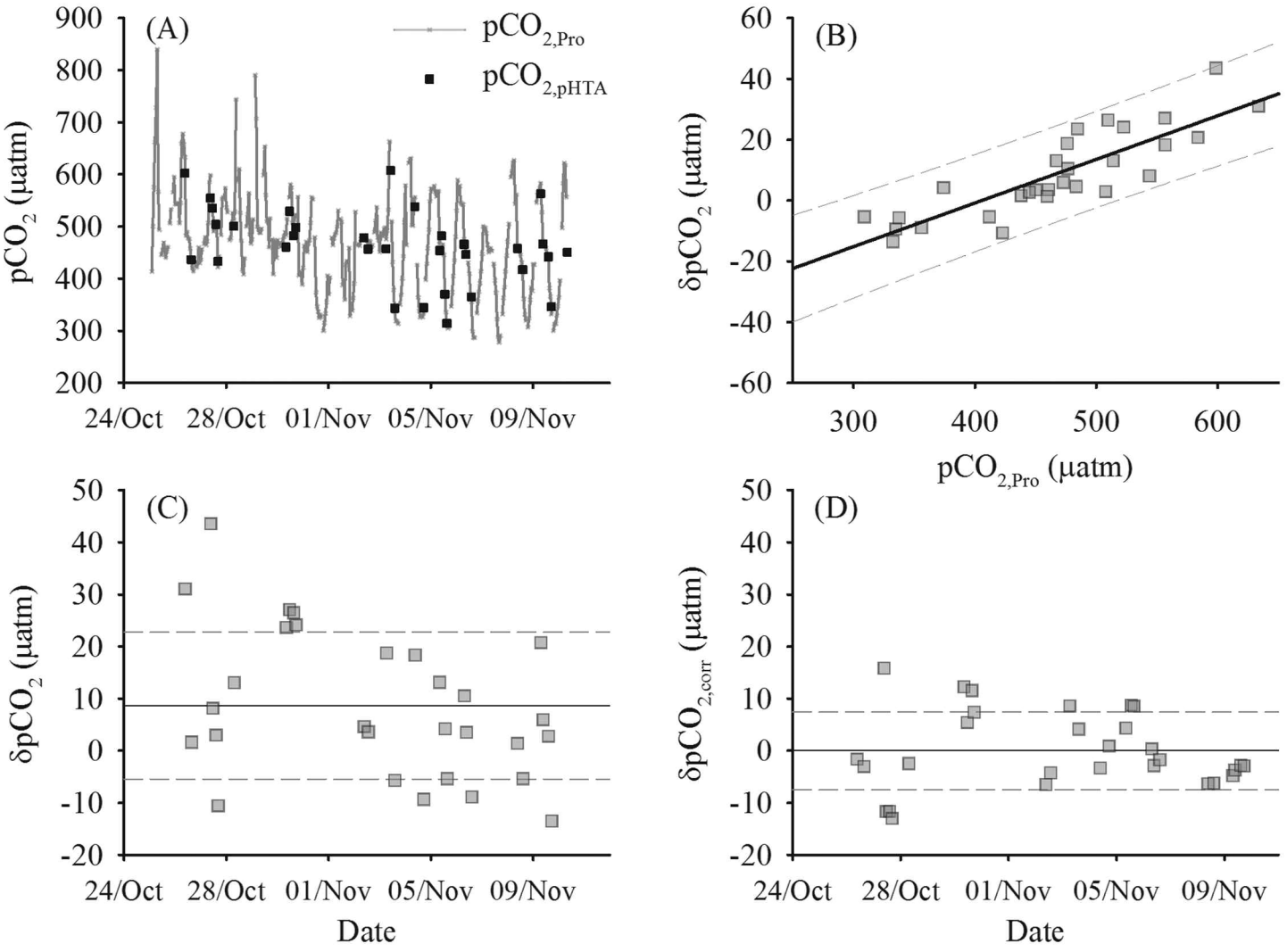

Fig. 2. The results of the ACT test in Kaneohe Bay: (A) the continuously hourly $pCO_{2,Pro}$ from the CO_2-Pro and the $pCO_{2,pHTA}$ calculated from discrete pH and TA; (B) the correlation between the δpCO_2 ($\delta pCO_2 = pCO_{2,Pro} - pCO_{2,pHTA}$) and $pCO_{2,Pro}$, the linear fit and the 95% prediction bands are shown; (C) δpCO_2 (8.4 ± 14.1 µatm) versus time; (D) $\delta pCO_{2,corr} = pCO_{2,ProCorr} - pCO_{2,pHTA}$ (0 ± 7.4 µatm) versus time, where $pCO_{2,ProCorr}$ is the sensor output corrected by $pCO_{2,pHTA}$ using the regression shown in panel B. Figure adapted from ACT (2009a).

units and the changing response of each unit before/after the recalibration in June 2010; 3) the influence of water patchiness, i.e., taking a discrete sample from a different water patch from that measured by the CO_2-Pro as the ship travelled at a relatively high speed (~15 knots). On the other hand, δpCO_2 values from successive transects using the same sensor generally do not differ greatly (e.g., transects 2, 3, 4 for sensor 47 and transects 7, 8, 9 for sensor 48, see Table 3). The changes in δpCO_2 among these successive transects may be mainly related to the changes in the condition of the gas transfer membranes. The values of δpCO_2 show a random distribution around the mean value for each transect except for transects 14 and 17 (Fig. 3C, D). The δpCO_2 in transect 14 shows a consistent increasing trend with time that may be associated with the contamination of the equilibrator or SNOMS tank (Fig. 3C). Moreover, values from the first 15 days of transect 17 (24.1 µatm) are significantly higher than those of the adjacent transects using the same sensor (2.6 and 7.4 µatm for transect 16 and 18, respectively), which is followed by a sudden decrease of ~40 µatm in δpCO_2 in the last 5 days (Fig. 3D). The causes of these dramatic changes in δpCO_2 during this particular transect are not well identified.

As the calculated $pCO_{2,DICTA}$ provides a consistent reference throughout the SNOMS operation for the two CO_2-Pro units before and after recalibration, we chose to correct $pCO_{2,Pro}$ against $pCO_{2,DICTA}$ for each transect individually. A time-dependent correction was applied to the transect 14, and the data in transect 17 are corrected in two sections as described above (Fig. 3C, D). As shown in Fig. 3B, the SD of the differences between the corrected sensor outputs and $pCO_{2,DICTA}$ is ±

Table 3. The mean and standard deviation (SD) of the differences in the CO_2-Pro outputs ($pCO_{2,Pro}$) and those calculated from DIC and TA ($pCO_{2,DICTA}$) during the SNOMS operation in the Pacific. R^2 refer to the correlation coefficients, and *n* is the number of the pairs of pCO_2.

Nr	Start port	End port	Start date	End date	Sensor	$pCO_{2,Pro} - pCO_{2,DICTA}$	SD	R^2	*n*
1	Taranga	Vancouver	23-Oct-09	11-Nov-09	48	5.7	9.8	0.91	14
2	Vancouver	Brisbane	02-Dec-09	25-Dec-09	48	failed measurement			
3	Taranga	Los Angeles	29-Jan-10	18-Feb-10	47	8.3	9.9	0.92	18
4	Los Angeles	Wellington	27-Mar-10	13-Apr-10	47	16.9	4.5	0.98	14
5	Taranga	Los Angeles	14-May-10	02-Jun-10	47	12.0	8.2	0.94	16
6	Vancouver	Auckland	25-Jun-10	14-Jul-10	48	failed measurement			
7	Taranga	Los Angeles	18-Aug-10	07-Sep-10	48	–6.6	8.6	0.97	19
8	Los Angeles	Brisbane	05-Oct-10	25-Oct-10	48	5.9	6.1	0.98	20
9	Taranga	Los Angeles	21-Nov-10	12-Dec-10	48	8.7	7.5	0.98	15
10	Los Angeles	Brisbane	18-Jan-11	12-Feb-11	none	no measurement; system removed for calibration			
11	Taranga	Los Angeles	16-Mar-11	10-Apr-11	none	no measurement; system removed for calibration			
12	Los Angeles	Brisbane	05-May-11	25-May-11	recalibrated 47	successful measurement; no DIC and TA data			
13	Taranga	Los Angeles	15-Jun-11	06-Jul-11	recalibrated 47	successful measurement; no DIC and TA data			
14	Los Angeles	Brisbane	30-Jul-11	20-Aug-11	recalibrated 47	0.3	18.0	0.85	18
15	Taranga	Los Angeles	20-Sep-11	09-Oct-11	recalibrated 47	6.6	8.3	0.94	15
16	Los Angeles	Brisbane	09-Nov-11	29-Nov-11	recalibrated 48	2.6	11.3	0.92	19
17	Taranga	Los Angeles	03-Jan-12	17-Jan-12	recalibrated 48	24.1	5.1	0.99	14
			18-Jan-12	23-Jan-12	recalibrated 48	–15.57 (sudden drop)	10.1		5
18	Los Angeles	Taranga	11-Feb-12	29-Feb-12	recalibrated 48	7.4	7.4	0.94	14

7.8 μatm (Fig. 3B), which is similar to the uncertainty of the calculation of $pCO_{2,DICTA}$ (± 8.1 μatm).

During the same period of the SNOMS transect 9, another SOO MV *Natalie Schulte* took pCO_2 measurement along the same route to that of the MV *Pacific Celebes*, but in a different direction (Fig. 4A). The pCO_2 measuring system was operated by Pacific Marine Environmental Laboratory (PMEL), which features a showerhead design of equilibrator and NDIR detection of dried gas (Pierrot et al. 2009). The availability of the regularly calibrated PMEL measurements (accuracy within 2 μatm) provided an opportunity for an intercomparison to evaluate the corrected SNOMS pCO_2 data. As shown in Fig. 4, the temperature, salinity, and pCO_2 measured by the two systems generally display the same latitudinal distributions. The elevated pCO_2 observed around the equator suggests the influence of westward advected CO_2-rich water originating from the equatorial upwelling (Fig. 4D). However, the difference in measuring time at the same location for the two ships ranges 0-16 d (ΔTime in Fig. 4). Therefore, the difference of the two pCO_2 measurements (Fig. 4F) includes not only the errors of the two measurements but also the natural spatial and temporal variability of pCO_2. The latter is related to water movement and warming/cooling of the surface water, which is indicated by the temperature and salinity differences between the two datasets (Fig. 4E).

To minimize the influence of natural pCO_2 variability on the comparison, the simultaneous measurements by the two systems were highlighted in Fig. 5. These measurements, with a time difference less than 0.5 d, were made in the equatorial region when the two ships were within 250 km of each other. The results measured by the two ships generally agreed in salinity (0.14 ± 0.05) and temperature (0.28 ± 0.09 °C, Fig. 5A). Previous time-series and Lagrangian observations in the equatorial Pacific show a diurnal pCO_2 variability of 2-8 μatm, which is mainly controlled by the temperature fluctuation (Goyet and Peltzer 1997; Degrandpre et al. 2004). To remove the temperature effect from the pCO_2 comparison, we normalize the $pCO_{2,Pro}$ to the temperature measured by the PMEL system. When the temperature effect is removed, the SNOMS pCO_2 values agree well with the PMEL measurements at –0.3 ± 3.9 μatm (δpCO_2 in Fig. 5B). This indicates reasonably good accuracy of the corrected SNOMS pCO_2 data (note that the raw CO_2-Pro outputs have been corrected against the carbonate calculation by 8.7 μatm, see Table 3).

Results of the Aquatron laboratory test

As shown in Fig. 6A, the water temperature during the Aquatron test generally showed a diurnal variability of 1-3°C and it varied within 15.5-17.5°C during the intercomparison period (Fig. 6A). The evaporation-induced increase in salinity was clearly observed and a sharp

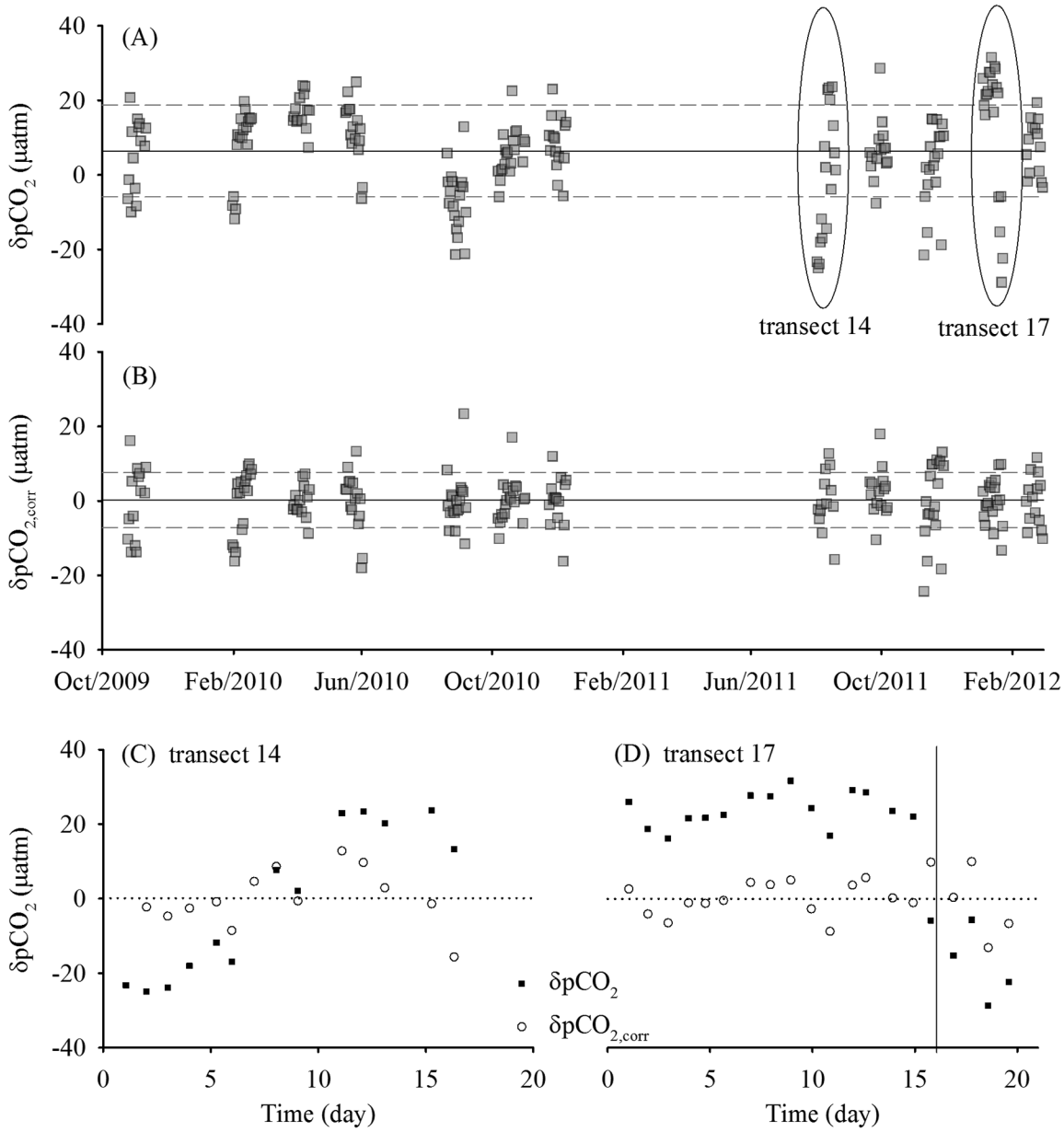

Fig. 3. For the 12 Pacific transects during the SNOMS operation, (A) $\delta pCO_2 = pCO_{2,Pro} - pCO_{2,DICTA}$, where $pCO_{2,Pro}$ is the raw sensor output and $pCO_{2,DICTA}$ is calculated from DIC and TA, the mean and SD of δpCO_2 are 6.4 ± 12.3 μatm; (B) $\delta pCO_{2,corr} = pCO_{2,ProCorr} - pCO_{2,DICTA}$, where $pCO_{2,ProCorr}$ is the $pCO_{2,Pro}$ corrected by $pCO_{2,pHTA}$ for individual transects, the mean and SD of $\delta pCO_{2,corr}$ are 0.2 ± 7.8 μatm. The increasing δpCO_2 in transect 14 and the sudden changes in δpCO_2 in transect 17 are shown in panel (C) and (D), together with the $\delta pCO_{2,corr}$.

salinity drop on 7 Aug indicates the substantial addition of the fresher harbor water after drainage from the sampling tube (Fig. 6A). To account for the changes in chemical properties due to evaporation, DIC and TA are normalized to the mean salinity 32.3: nX = (X/Salinity) × 32.3, where X is the measured concentration of DIC or TA, and nX is the salinity-normalized concentration (Fig. 6D). During the stabilization period, pCO_2 decreased from the initial value (up to 900 μatm) to a relative constant range within 640-690 μatm (Fig. 6C). At the same time, DIC and TA both showed an increasing trend (Fig. 6B) whereas the concentrations of nutrients remained at low levels with little variability (Fig. 6E, F). The relatively constant nDIC (~2150 μmol kg^{-1}, Fig. 6D) suggests that the increase in DIC (Fig. 6B) mainly resulted from evaporation. In contrast, the salinity-normalized nTA increased significantly from 2240 to 2290 μmol kg^{-1} (Fig. 6D). During the intercomparison period, the pCO_2 levels were adjusted to be in the "natural" open ocean range of 300-550 μatm by the bubbling of CO_2-free air (started on 10 Jul, 2 Aug, and 31 Aug). Corresponding decreases in pCO_2 and DIC (Fig. 6B, C) were

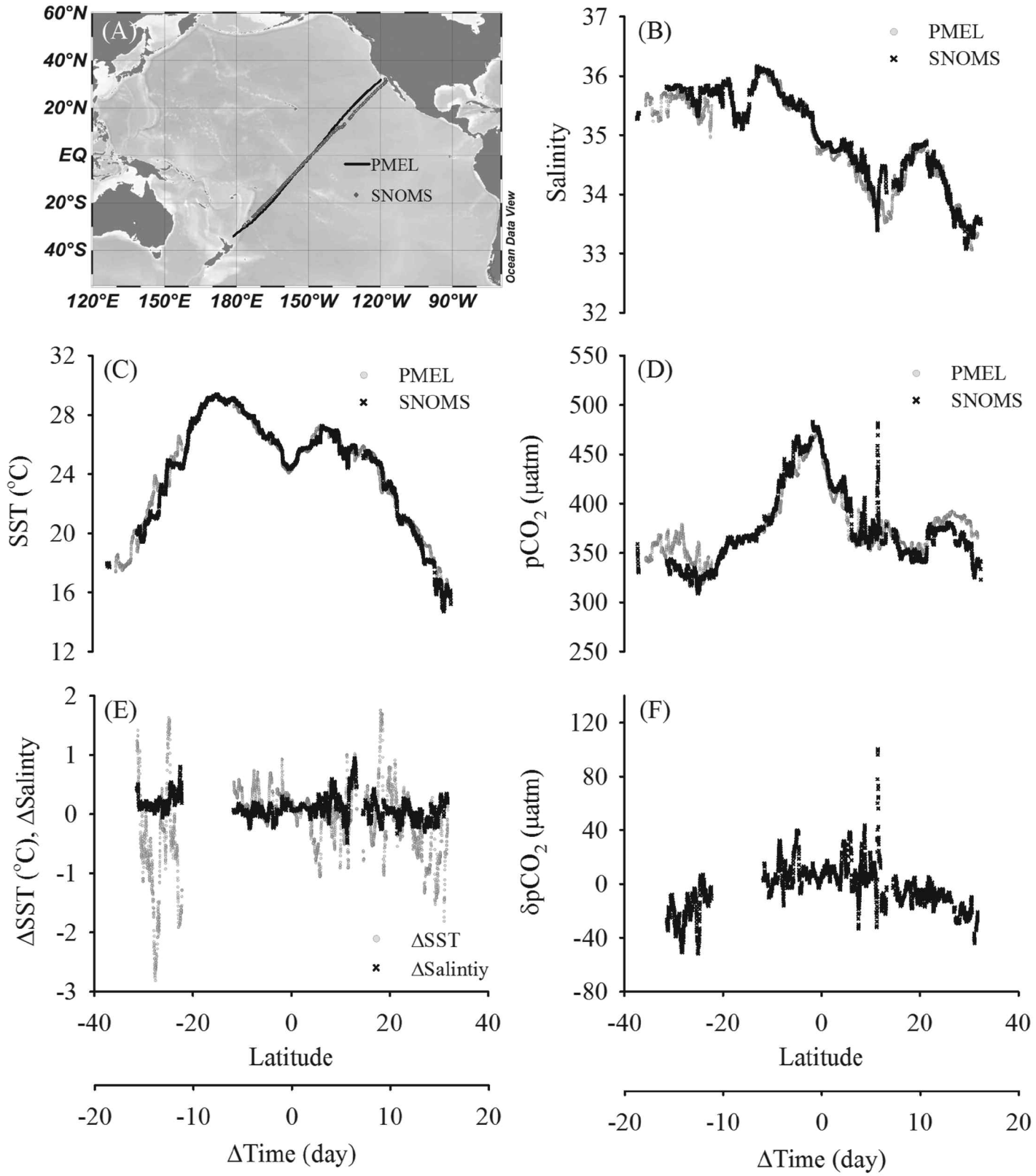

Fig. 4. (A) The overlapping route of the two ships of opportunity; the latitudinal distributions of (B) salinity, (C) SST, (D) pCO_2 measured by the PMEL and SNOMS systems; and their differences in (E) SST, salinity, and (F) pCO_2. ΔTime is the difference in measuring time at the same location for the two ships.

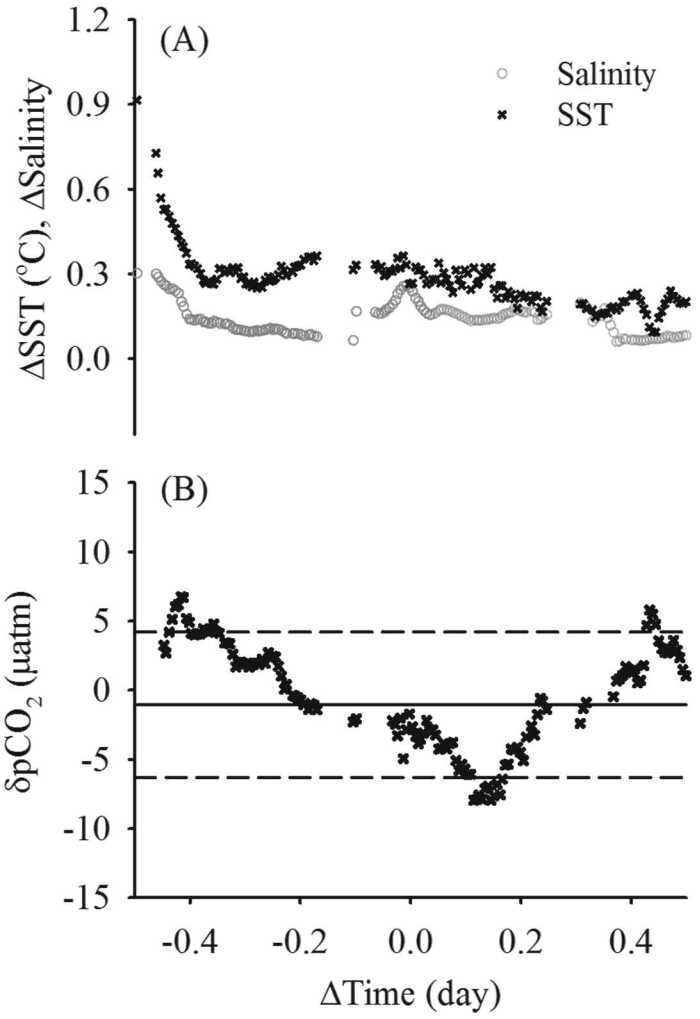

Fig. 5. The differences of the simultaneous measurements (time difference less than 0.5 d and distance within 250 km) by the SNOMS and PMEL systems: (A) SST and salinity; (B) pCO_2.

observed when the tank was purged with CO_2-free air, which was followed by progressive increases after the bubbling stopped. On 7 Aug, the dramatic changes in all measured variables were caused by the substantial addition of newly pumped water as described above. This induced sudden decreases in salinity, TA, and DIC (Fig. 6A, B) that were associated with increases in pCO_2 and nutrients (Fig. 6C, E, F).

The intercomparison of the pCO_2 measurements by the SNOMS and NOIZ systems is presented in Fig. 7. The CO_2-Pro functioned properly throughout the Aquatron test while the NOIZ system suffered from malfunctions on a few occasions (the failed measurements are not included in the intercomparison, Fig. 7A). Both measurements were averaged to 5 min interval and $pCO_{2,NOIZ}$ was normalized to the temperature in the SNOMS tank to eliminate temperature influence on the comparison (the average temperature difference is ~0.08 °C, which corresponds to ~1.5 μatm in pCO_2). There may be a slight delay in $pCO_{2,Pro}$ when responding to the pCO_2 disturbances (bubbling, water top up) as these events occurred in the Aquatron tank were first observed by the NOIZ system. Overall, the pCO_2 measured by the two systems shows a tight correlation ($pCO_{2,Pro}$ = 0.9987 × $pCO_{2,NOIZ}$, R^2 = 0.99, not shown). The mean and SD of the differences between the two measurements ($\delta pCO_2 = pCO_{2,Pro} - pCO_{2,NOIZ}$) are –3.0 ± 4.4 μatm ($n$ = 13847, Fig. 7C). δpCO_2 does not show a constant drift over the two month test (Fig. 7C) but appears to vary with the absolute pCO_2 concentration (Fig. 7B), which may be due to a linear error in the sensor calibration. When the CO_2-Pro measurements are calibrated against $pCO_{2,NOIZ}$, the differences between the calibrated $pCO_{2,ProCorr}$ and $pCO_{2,NOIZ}$ ($\delta pCO_{2,corr}$ in Fig. 7D, 0 ± 2.9 μatm) show a random distribution around the mean value throughout the intercomparison experiment, which suggests no instrumental drift of the CO_2-Pro occurred during the two-month period.

An interesting phenomenon observed in the Aquatron test is the unexpected changes in alkalinity. The increase in nTA during the stabilization period (2240 to 2290 μmol kg^{-1}, Fig. 6D) cannot be explained by the changes in inorganic carbon content and nutrients: (1) the small changes in nDIC and nutrients indicate minor TA changes resulted from biological activities, such as precipitation and dissolution of $CaCO_3$ (which changes TA and DIC at a ratio of 2:1) and nutrient uptake and release by algae (which changes TA following the nutrient-H^+-compensation principle) (Wolf-Gladrow et al. 2007); (2) air-sea gas exchange of CO_2 changes DIC but does not affect the concentration of TA (Wolf-Gladrow et al. 2007); (3) the oxygen saturation varied between 86-104% (not shown), which suggests no TA changes induced by anaerobic processes. Similarly, increases in nTA observed after the top up event on 7 Aug (2270 to 2290 μmol kg^{-1}) also did not match the changes in nDIC and nitrates: the increasing concentrations of nDIC and nitrates during this period (Fig. 6D, E) suggests the occurrence of remineralization processes which would decrease TA.

To examine the TA anomaly in the Aquatron test, we calculate alkalinity from the measured DIC and pCO_2 using the CO2SYS. The calculated Alk_{sys} (uncertainty estimated to be ± 3.5 μmol kg^{-1}) is the alkalinity expected at the equilibration state of the carbonate system, which accounts for the major inorganic buffering acid-base pairs. It is shown in Fig. 8A that the concentrations of Alk_{sys} are 3–24 μmol kg^{-1} lower than the measured values of TA_{meas}. This excess of TA_{meas} over the Alk_{sys} (Alk_{excess}) suggests substances or processes, which affect the concentration of alkalinity and/or the titration process of alkalinity. This may be due to waste water or reactive particles in the harbor, contamination during the pumping process, reaction with the fiberglass wall of the Aquatron tank, or the existence of organic alkalinity. Although we cannot clearly identify the source(s) of the alkalinity anomaly, it is shown that using the measured TA_{meas} for carbonate calculation would result in underestimates in pCO_2 (Fig. 8B). The

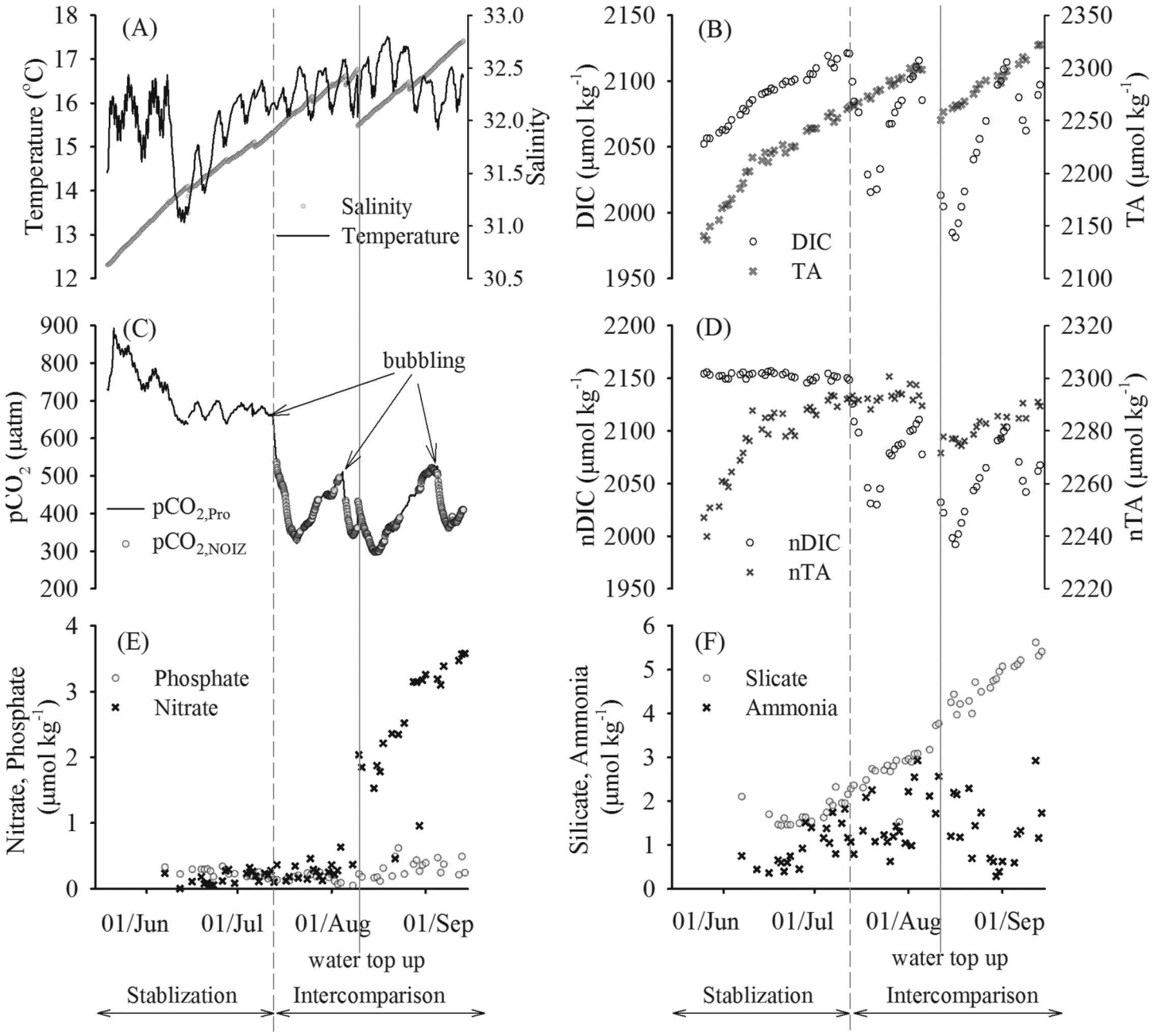

Fig. 6. The variations of (A) temperature and salinity, (B) DIC and TA, (C) pCO_2 measured by the CO_2-Pro and the NOIZ system, (D) salinity normalized nDIC and nTA, (E) nitrate and phosphate, and (F) silicate and ammonia during the Aquatron test. The dashed line and the solid line correspond to the starting of the intercomparison and the substantial water top up event, respectively. The arrow lines in panel (C) correspond to the starting of the bubbling of the CO_2-free gas. See the text for details.

$pCO_{2,DICTA}$ calculated from TA_{meas} and DIC is 7-90 μatm lower compared with direct pCO_2 measurement, and this underestimation ($pCO_{2,bias}$= $pCO_{2,Pro}$ - $pCO_{2,DICTA}$) shows a similar trend to that of Alk_{excess} (Fig. 8C). Closer investigation shows that the percentage bias in pCO_2 (%$pCO_{2,bias}$= $pCO_{2,bias}$/$pCO_{2,Pro}$) is positively correlated to the percentage bias in alkalinity (%Alk_{excess}= Alk_{excess}/TA_{meas} =12.54 × %$pCO_{2,bias}$, Fig. 8D).

Results of the long-term in situ operation on the PAP mooring

Since the first deployment in June 2010, a CO_2-Pro continuously worked at the PAP site until Jan 2011 when a communication cable of the hub controller broke. A calibrated unit replaced the original sensor in July 2011 and operated until March 2012 when the controlling hub was flooded. A frustratingly short deployment during May to July 2012 was due to communication failure when the sensor frame became

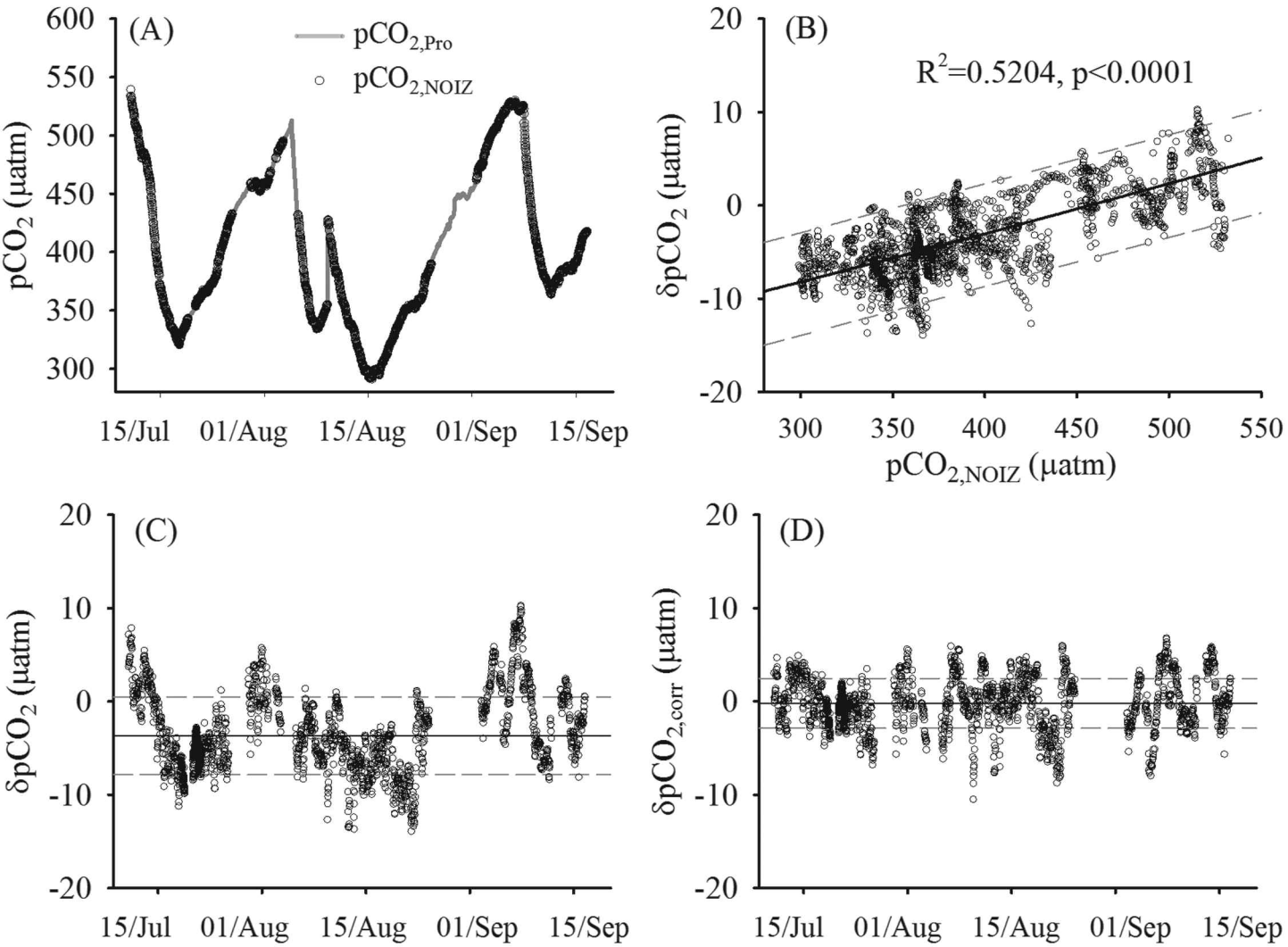

Fig. 7. The results of the two-month intercomparison between the CO_2-Pro and the calibrated NOIZ system: (A) pCO_2; (B) the pCO_2 differences (δpCO_2 = $pCO_{2,Pro}$ – $pCO_{2,NOIZ}$) versus $pCO_{2,NOIZ}$, the linear fit and the 95% prediction bands are shown; (C) δpCO_2 versus time; (D) $\delta pCO_{2,corr}$ is the pCO_2 differences between the corrected $pCO_{2,Pro}$ and $pCO_{2,NOIZ}$.

detached from the mooring. The deployment of the CO_2-Pro at PAP was successful for up to 7 months while the failure of longer measurement was due to problems of the hub controller rather than the sensor malfunction.

In contrast to continuous measurement on SOO, the CO_2-Pro on the PAP mooring was operated intermittently (1-4 times a day) due to the limited power supply. Each measurement lasted for 45-120 min, which assures full equilibrium with the seawater (typically within 15 min). The pCO_2 of the oligotrophic surface water around the PAP site is expected to show minor variability during the short duration of each measurement. However, the pCO_2 measured by the CO_2-Pro showed a consistent increase throughout each measurement (Fig. 9A presents a typical measuring cycle of the CO_2-Pro) while the in situ temperature and salinity remained unchanged (not shown). It is noted that the optical cell temperature of the detector shows an increasing trend similar to that of pCO_2 (Fig. 9A). Moreover, the cell temperature during the measurement (t_{meas}) is found to be much higher than that during the ZPC ($\Delta t_{cell} = t_{meas} - t_{ZPC}$, Fig. 9A). As the NDIR measurement is affected by the optical cell temperature, this temperature fluctuation would result in errors in pCO_2 detection.

To examine the influence of optical cell temperature, a laboratory test was carried out when the sensor was recovered from deployment. A series of CO_2 standard gases (256, 363, and 459 ppm) were connected to the detector bypassing the equilibrator for direct NDIR measurements. In addition, a CO_2-free gas (N_2 passing through CO_2 absorbance) was used to simulate the baseline measurement of C_{zero} during the ZPC. Measurements of these gases were carried out following a ZPC at 40°C, whereas the temperature of the optical cell during the

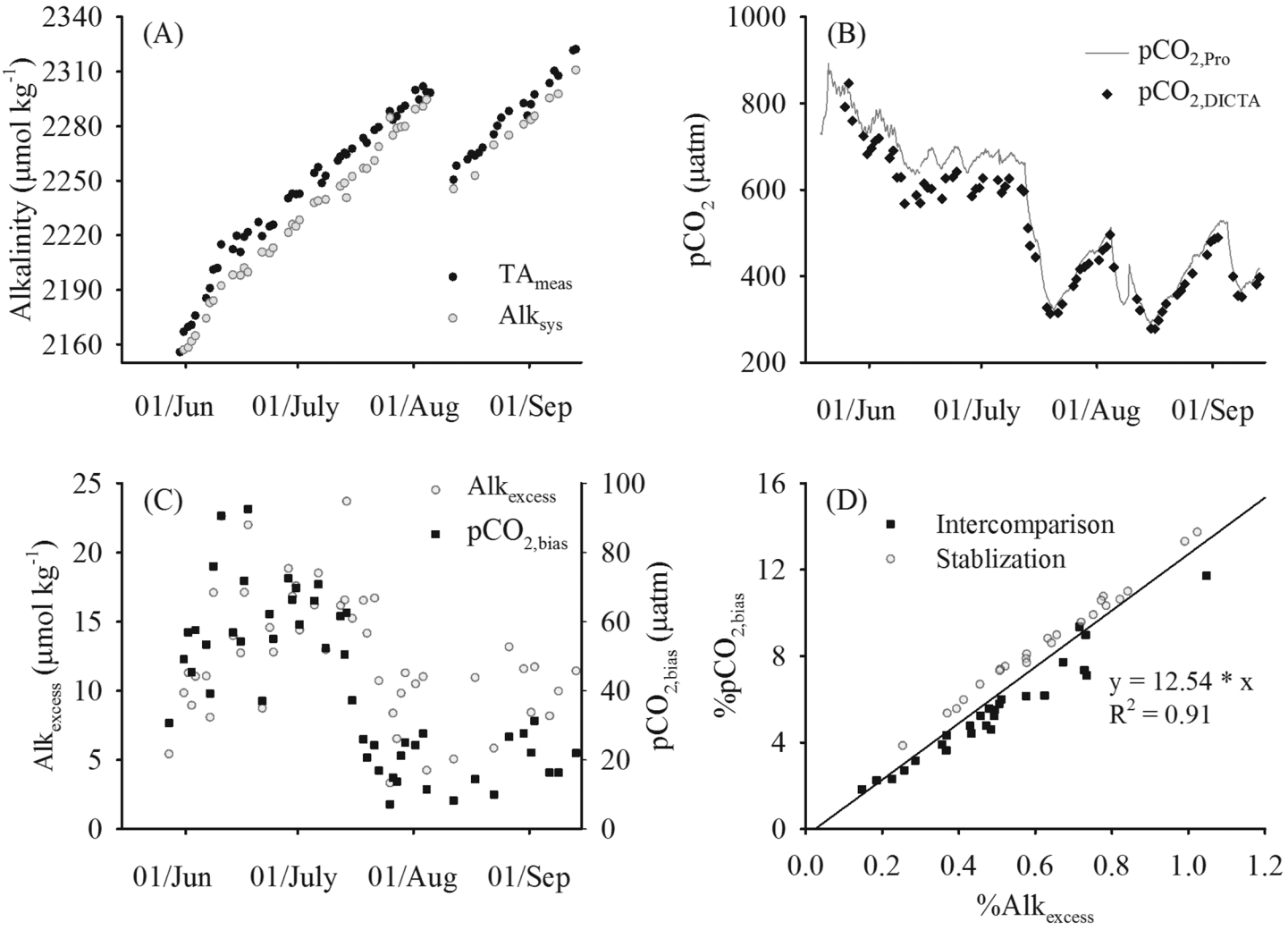

Fig. 8. (A) The concentrations of TA_{meas} from direct measurement and Alk_{sys} calculated from the measured DIC and pCO_2; (B) pCO_2 measured by the CO_2-Pro ($pCO_{2,Pro}$) and $pCO_{2,DICTA}$ calculated from the measured DIC and TA; (C) the differences of TA and pCO_2 between direct measurements and the carbonate calculations ($Alk_{excess} = TA_{meas} - Alk_{sys}$, $pCO_{2,bias} = pCO_{2,Pro} - pCO_{2,DICTA}$); (D) the correlation between the percentage of $pCO_{2,bias}$ and Alk_{excess} in comparison to the measured values ($\%pCO_{2,bias} = pCO_{2,bias} / pCO_{2,Pro}$, $\%Alk_{excess} = Alk_{excess}/TA_{meas}$).

measurement of each gas was perturbed by heating with an electric fan and cooling with a cold pack (Δt_{cell} was adjusted to be –0.7 to 1.8°C). The test results show that the inferred signals of all measured gases decrease linearly with increasing optical cell temperature (not shown). As the zero-CO_2 signal also changes with temperature, using a baseline measured at t_{zero} as the blank reference for measurements at different cell temperatures would result in errors in calculating ε and xCO_2. As shown in Fig. 9B, the errors in xCO_2 ($xCO_{2,error}$ = measured xCO_2 – certified value) were linearly correlated with Δt_{cell}, and the temperature effects are similar for the three standard gases at 15 ppm °C^{-1}. It is also shown that the errors in xCO_2 can be removed if the influence of Δt_{cell} is considered in the calculations of ε and xCO_2 (Fig. 9B). The scatter of the data should mainly be caused by the uneven heating or cooling on the optical cell in our test.

When this correction of Δt_{cell} is applied to the PAP measurement, the corrected $pCO_{2,tcorr}$ stabilizes at 15 min after the ZPC as expected from the equilibrium time and shows minor changes afterward (Fig. 9A). It is notable that the Δt_{cell} at the PAP mooring is quite large (up to 1.5°C), which corresponds to an error in pCO_2 as large as 25 μatm. This is because of the early ZPC at low t_{ZPC} when the optical cell was not sufficiently warmed up, as well as inadequate thermostat control of the optical cell, i.e., the cell temperature continued to increase after the ZPC. In contrast, this issue is not significant for the continuous measurements as the long-term operation allows the optical cell to be fully warmed up minimizing the temperature difference between ZPC and measurement. The Δt_{cell} during the SNOMS and Aquatron operations was ~ 0.2°C corresponding to an error of 3 μatm in pCO_2; corrections of Δt_{cell} are applied to the SNOMS and Aquatron data before assessment.

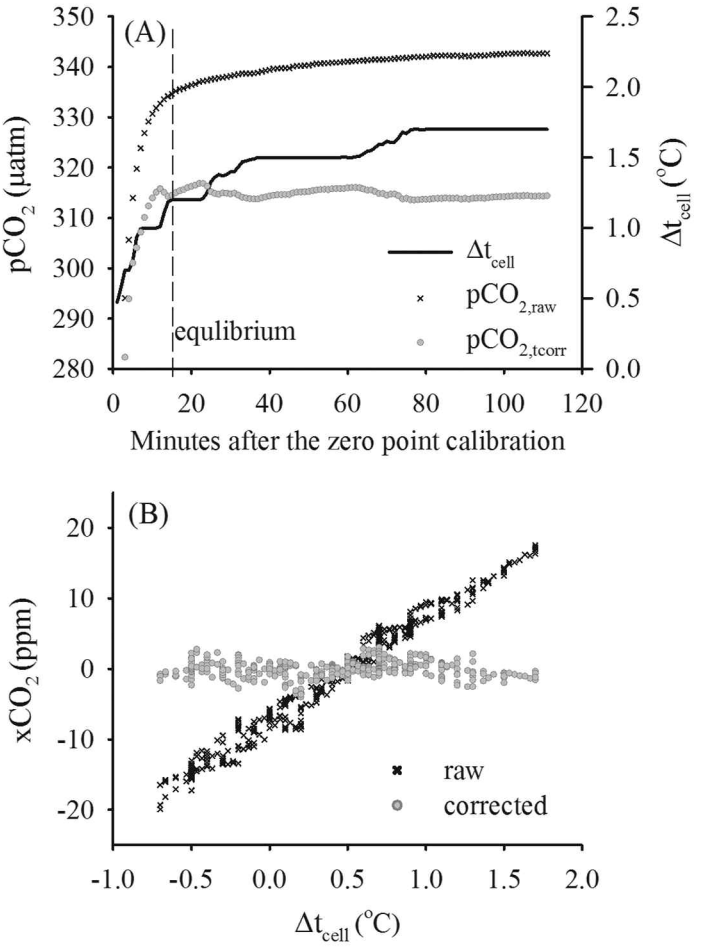

Fig. 9. (A) A typical measuring cycle of the CO_2-Pro on the PAP mooring, Δt_{cell} is the optical cell temperature deviation during the measurement compared to that during the zero point calibration, $pCO_{2,raw}$ and $pCO_{2,tcorr}$ are the raw sensor outputs and those corrected for the influence of Δt_{cell}; (B) the errors in xCO_2 measurements resulting from Δt_{cell} for the three standard gases in the laboratory test, and those after correction for the temperature influence. See the text for details.

Discussion, recommendations, and improvements

Overall, the CO_2-Pro is a very robust sensor suitable for onboard and in situ measurements on platforms with limited working space and on platforms that cannot be serviced regularly. The sensor's capacity for long-term operation is demonstrated by the successes of the SNOMS operation and PAP mooring deployments. In this study, the performance of the CO_2-Pro is evaluated extensively under field and laboratory conditions, and the results are summarized in Table 4. The CO_2-Pro agreed with a calibrated water-air equilibrator system during a 2-month side-by-side laboratory intercomparison (–3.0 ± 4.4 μatm). When used at sea, the direct sensor outputs differed from the calculated pCO_2 reference by 6.4 ± 12.3 μatm on a SOO and 8.7 ± 14.1 μatm on a mooring. These differences result from a number of factors including the uncertainties in the reference and the comparison process, the sensor error, how well the sensor was set up, contamination issues, etc. Our study suggests that, when pCO_2 references are available for correction, the uncertainty of the corrected sensor result is similar to and largely determined by the uncertainties of the references.

One significant limitation of the CO_2-Pro is the lack of regular calibration against standard gases, which makes it difficult to assess the accuracy of the measurement when it is deployed alone. To remedy this potential problem, Pro-Oceanus has introduced a new version of CO_2-Pro with onboard control of a gas port for introduction of standard gases. If the CO_2-Pro is to be used for onboard or laboratory measurements, this version, which enables external manual calibration is recommended for use. In the future, an automatic calibration function using standard gases would be highly desired to optimize the accuracy of the measurement. For the field applications, users of the CO_2-Pro (and any chemical sensor that is not calibrated while deployed) should calibrate the sensor before and after long-term deployments to examine any potential drift. Collection of discrete samples over a wide range of pCO_2 concentrations for the determination of other carbonate variables is recommended to provide quality control on the sensor, and also, to provide additional information on biogeochemical variability.

Clearly, the accuracy of the calibration gases used in the original factory calibration and any subsequent recalibrations is a critical factor in sensor accuracy. However, this study reveals that some inaccuracy of the sensor may be caused by calibration error, which may be related to the quality of calibration gases used. To address this problem, Pro-Oceanus has performed all factory calibrations using NOAA and NOAA-traceable standard gases that are accurate to better than ±1 ppm since 2011. Moreover, our study reveals that error in pCO_2 measurement of the CO_2-Pro can result from the changes in optical cell temperature between the ZPC and measurement. This problem may be significant for the early versions of CO_2-Pro whose optical cells are not well thermostatically controlled. However, this error is correctable and can be avoided by better temperature control on the detector optical cell. Since 2011, an improved temperature control is a standard feature of CO_2-Pro which stabilizes the fluctuation of the temperature of the detector cell to within ± 0.05°C.

To fulfill the target of constraining the regional air-sea CO_2 fluxes to 0.2 Pg C y^{-1}, pCO_2 measuring systems need to be accurate to within 2 μatm for seawater pCO_2 (Pierrot et al. 2009). This is presently a demanding requirement for pCO_2 sensors. As demonstrated in this work, the CO_2-Pro sensors that were tested (particularly the older versions) did not meet the gold standard of 2 μatm. However, recent improvements to the CO_2-Pro (as mentioned above) should enhance sensor performance. Considering the large variability of pCO_2 in time and space, there is great value in expanding in situ observations by using sensors with a known reasonably good accuracy. The developing sensor technology provides a very effec-

Table 4. Summary of the assessment results of the CO_2-Pro in this study.

	Application	Mode	Time length	Reference and its uncertainty	Difference with the reference (μatm) Direct output	Corrected output
ACT	mooring test	in situ	16 d	calculation from pH and TA (±7.5 μatm)	8.7 ± 14.1	0 ± 7.4
SNOMS	SOO observation	underway	several months	calculation from DIC and TA (±8.1 μatm)	6.4 ± 12.3	0.2 ± 7.8
				direct and calibrated measurement (±2 μatm)		–0.3 ± 3.9
Aquatron	laboratory test	underway	2 months	direct and calibrated measurement (±2 μatm)	–3.0 ± 4.4	0 ± 2.9

tive way to increase the capability for global and regional ocean monitoring. This can provide useful information on the surface ocean where no or few measurements have been made or other extreme marine environments such as in the deep ocean (the CO_2-Pro has been successfully used on the SeaCycler and NEPTUNE profilers, B. Johnson pers. comm.) or near hydrothermal vents (Nakano et al. 2006; Willcox et al. 2009). Moreover, the long-term time series data from fixed-station sensor deployments provides a most powerful tool to understand the controlling mechanisms regulating the changes in ocean CO_2.

Another interesting finding in this study is the alkalinity anomaly and the mismatch in carbonate calculation in the Aquatron test. Excess of measured TA (up to 24 μmol kg^{-1}) are found in comparison with that calculated from DIC and pCO_2, whereas the carbonate calculation of pCO_2 using measured TA and DIC result in underestimation in pCO_2 (up to 90 μatm). Although the causes of this TA anomaly cannot be confirmed in our study, one possible explanation is the organic contribution to alkalinity. Many previous studies have proved the existent of organic alkalinity in both laboratory cultures (up to 800 μmol kg^{-1}) and natural coastal environments (tens of μmol kg^{-1}) (Cai et al. 1998; Hernández-Ayón et al. 2007; Muller and Bleie 2008; Kim and Lee 2009). Since the use of alkalinity including organic bases could lead to errors in the carbonate calculation, care should be taken when making calculations for the marine carbonate system in environments with high concentration of organic matter, e.g. estuary, coastal water, and incubation culture solution. When studying the organic matter-rich waters, alkalinity is recommended to be measured using method proposed by Cai et al. (1998) or Hernández-Ayón et al. (1999) to identify the organic alkalinity.

Acknowledgment

The Swire Charitable Trust and the Swire Education Trust are gratefully acknowledged for funding the Swire NOCS Ocean Monitoring System (SNOMS) project and the scholarship for Zong-Pei Jiang's PhD study. LDEO contribution number 7768. The Swire Group Company China Navigation and the crews on the MV *Pacific Celebes* are to be thanked for supporting the operation of the SNOMS project. Dave Childs provided invaluable analysis of the salinity samples at NOCS. At the Institute of Ocean Science in Canada, Marty Davelaar, Jim Christian, and Kyle Davidson helped with sample pickups and joined in the SNOMS sample processing exercise. We gratefully thank Jim Eddington, Emily Chua, Claire Normandeau, Trina Whitsitt, and Douglas Schillinger during the Aquatron tests at Dalhousie University. We also thank the support from Richard Lampitt, Kate Larkin, Maureen Pagnani, Thanos Gkritzalis on the sensor deployment and maintenance at the PAP site. Wei-Jun Cai is thanked for the helpful discussion on the organic alkalinity. We also thank Mike DeGrandpre and Wiley Evans for their helpful suggestions on improving this paper.

References

ACT. 2009a. Performance demonstration statement ProOceanus Systems Inc. PSI CO2-ProTM. Alliance for Coastal Technologies, report Ref.No. ACT TD10-03.

———. 2009b. Protocols for demonstrating the performance of in situ pCO2 analyzers. Alliance for Coastal Technologies, report Ref.No. ACT PD09-01.

Bakker, D. C. E., and others. 2013. An update to the surface ocean CO_2 atlas (SOCAT version 2). Earth System Science Data Discussions 6:465-512 [doi:10.5194/essdd-6-465-2013].

Bates, N. R. 2002. Seasonal variability of the effect of coral reefs on seawater CO_2 and air-sea CO_2 exchange. Limnol. Oceanogr. 47:43-52 [doi:10.4319/lo.2002.47.1.0043].

———. 2007. Interannual variability of the oceanic CO2 sink in the subtropical gyre of the North Atlantic Ocean over the last 2 decades. J. Geophys. Res. 112: C09013. [doi: 10.1029/2006jc003759].

Beggs, H. M., R. Verein, G. Paltoglou, H. Kippo, and M. Underwood. 2012. Enhancing ship of opportunity sea surface temperature observations in the Australian region. J. Oper. Oceanogr. 5:59-73.

Borges, A. V., and M. Frankignoulle. 1999. Daily and seasonal variations of the partial pressure of CO_2 in surface seawater along Belgian and southern Dutch coastal areas. J. Mar. Syst. 19:251-266 [doi:10.1016/S0924-7963(98)00093-1].

Cai, W. J., Y. C. Wang, and R. E. Hodson. 1998. Acid-base properties of dissolved organic matter in the estuarine waters of Georgia, USA. Geochim. Cosmochim. Acta 62:473-483 [doi:10.1016/S0016-7037(97)00363-3].

Dai, M. H., and others. 2009. Diurnal variations of surface sea-

water pCO_2 in contrasting coastal environments. Limnol. Oceanogr. 54:735-745 [doi:10.4319/lo.2009.54.3.0735].

De La Paz, M., A. Gomez-Parra, and J. Forja. 2008. Tidal-to-seasonal variability in the parameters of the carbonate system in a shallow tidal creek influenced by anthropogenic inputs, Rio San Pedro (SW Iberian Peninsula). Cont. Shelf Res. 28:1394-1404 [doi:10.1016/j.csr.2008.04.002].

Degrandpre, M. D. 1993. Measurement of seawater pCO_2 using a renewable-reagent fiber optic sensor with colorimetric detection. Anal. Chem. 65:331-337 [doi:10.1021/ac00052a005].

———, T. R. Hammar, S. P. Smith, and F. L. Sayles. 1995. In situ measurements of seawater pCO_2. Limnol. Oceanogr. 40:969-975 [doi:10.4319/lo.1995.40.5.0969].

———, ———, and C. D. Wirick. 1998. Short-term pCO_2 and O_2 dynamics in California coastal waters. Deep Sea Res. II 45:1557-1575 [doi:10.1016/S0967-0645(98)80006-4].

———, M. M. Baehr, and T. R. Hammar. 1999. Calibration-free optical chemical sensors. Anal. Chem. 71:1152-1159 [doi:10.1021/ac9805955].

———, R. Wanninkhof, W. R. Mcgillis, and P. G. Strutton. 2004. A Lagrangian study of surface pCO_2 dynamics in the eastern equatorial Pacific Ocean. J. Geophys. Res. 109:C08S07 [doi:10.1029/2003JC002089].

Dickson, A. G. 1990. Standard potential of the (AgCl(s) + 1/2 H2(g) = Ag(s) + HCl(aq)) cell and the dissociation constant of bisulfate ion in synthetic sea water from 273.15 to 318.15 K. J. Chem. Thermodyn. 22:113-127 [doi:10.1016/0021-9614(90)90074-Z].

———, C. L. Sabine, and J. R. Christian. 2007. Guide to best practices for ocean CO_2 measurements. North Pacific Marine Science Organization (PICES).

Doney, S. C., and others. 2009. Surface-ocean CO_2 variability and vulnerability. Deep Sea Res. II 56:504-511 [doi:10.1016/j.dsr2.2008.12.016].

Fiedler, B., P. Fietzek, N. Vieira, P. Silva, H. C. Bittig, and A. Körtzinger. 2012. In situ CO_2 and O_2 measurements on a profiling float. J. Atmos. Oceanic Technol. 30:112-126 [doi:10.1175/JTECH-D-12-00043.1].

Goyet, C., D. R. Walt, and P. G. Brewer. 1992. Development of a fiber optic sensor for measurement of pCO_2 in sea water: design criteria and sea trials. Deep Sea Res. I 39:1015-1026 [doi:10.1016/0198-0149(92)90037-T].

———, and E. T. Peltzer. 1997. Variation of CO_2 partial pressure in surface seawater in the equatorial Pacific Ocean. Deep Sea Res. I 44:1611-1625 [doi:10.1016/S0967-0637(97)00037-X].

Hartman, S. E., and others. 2012. The Porcupine Abyssal Plain fixed-point sustained observatory (PAP-SO): variations and trends from the Northeast Atlantic fixed-point time-series. ICES J. Mar. Sci. 69:776-783 [doi:10.1093/icesjms/fss077].

Hernández-Ayón, J. M. N., S. L. Belli, and A. Zirino. 1999. pH, alkalinity and total CO_2 in coastal seawater by potentiometric titration with a difference derivative readout. Anal. Chim. Acta 394:101-108 [doi:10.1016/S0003-2670(99)00207-X].

———, A. Zirino, A. G. Dickson, T. Camiro-Vargas, and E. Valenzuela-Espinoza. 2007. Estimating the contribution of organic bases from microalgae to the titration alkalinity in coastal seawaters. Limnol. Oceanogr. Methods 5:225-232 [doi:10.4319/lom.2007.5.225].

Hydes, D. J., and others. 2013. Report of the SNOMS Project 2006 to 2012, SNOMS: SWIRE NOCS Ocean Monitoring System. Part 1: Narrative description. National Oceanography Centre Research and Consultancy Report, 33.

Jiang, Z.-P., and others. 2011. Short-term dynamics of oxygen and carbon in productive nearshore shallow seawater systems off Taiwan: Observations and modeling. Limnol. Oceanogr. 56:1832-1849 [doi:10.4319/lo.2011.56.5.1832].

———, and others. 2013. Key controls on the seasonal and interannual variations of the carbonate system and air-sea CO_2 flux in the Northeast Atlantic (Bay of Biscay). J. Geophys. Res. 118:1-16.

Kayanne, H., and others. 2002. Submergible system to measure seawater pCO_2 on a shallow sea floor. Mar. Technol. Soc. J. 36:23-28 [doi:10.4031/002533202787914241].

Kim, H.-C., and K. Lee. 2009. Significant contribution of dissolved organic matter to seawater alkalinity. Geophys. Res. Lett. 36:L20603 [doi:10.1029/2009GL040271].

Körtzinger, A., H. Thomas, B. Schneider, N. Gronau, L. Mintrop, and J. C. Duinker. 1996. At-sea intercomparison of two newly designed underway pCO_2 systems - encouraging results. Mar. Chem. 52:133-145 [doi:10.1016/0304-4203(95)00083-6].

Lee, S. S., C. Park, P. Fenter, N. C. Sturchio, and K. L. Nagy. 2010. Competitive adsorption of strontium and fulvic acid at the muscovite–solution interface observed with resonant anomalous X-ray reflectivity. Geochim. Cosmochim. Acta 74:1762-1776 [doi:10.1016/j.gca.2009.12.010].

Lefévre, N., J. P. Ciabrini, G. Michard, B. Brient, M. Duchaffaut, and L. Merlivat. 1993. A new optical sensor for pCO_2 measurement. Mar. Chem. 42:189-198 [doi:10.1016/0304-4203(93)90011-C].

Lu, Z., M. Dai, K. Xu, J. Chen, and Y. Liao. 2008. A high precision, fast response, and low power consumption in situ optical fiber chemical pCO_2 sensor. Talanta 76:353-359 [doi:10.1016/j.talanta.2008.03.005].

Mehrbach, C., C. H. Culberson, J. E. Hawley, and R. M. Pytkowicz. 1973. Measurement of the apparent dissociation constants of carbonic acid in seawater at atmospheric pressure. Limnol. Oceanogr. 18:897-907 [doi:10.4319/lo.1973.18.6.0897].

Millero, F. J., T. B. Graham, F. Huang, H. Bustos-Serrano, and D. Pierrot. 2006. Dissociation constants of carbonic acid in seawater as a function of salinity and temperature. Mar. Chem. 100:80-94 [doi:10.1016/j.marchem.2005.12.001].

Mojica Prieto, F. J., and F. J. Millero. 2002. The values of pK1 + pK2 for the dissociation of carbonic acid in seawater.

Geochim. Cosmochim. Acta 66:2529-2540 [doi:10.1016/S0016-7037(02)00855-4].

Muller, F. L. L., and B. Bleie. 2008. Estimating the organic acid contribution to coastal seawater alkalinity by potentiometric titrations in a closed cell. Anal. Chim. Acta 619:183-191 [doi:10.1016/j.aca.2008.05.018].

Nakano, Y., H. Kimoto, S. Watanabe, K. Harada, and Y. W. Watanabe. 2006. Simultaneous vertical measurements of in situ pH and CO_2 in the sea using spectrophotometric profilers. J. Oceanogr. 62:71-81 [doi:10.1007/s10872-006-0033-y].

Nemoto, K., and others. 2009. Continuous observations of atmospheric and oceanic CO2 using a moored buoy in the East China Sea: Variations during the passage of typhoons. Deep Sea Res. II 56:542-553 [doi:10.1016/j.dsr2.2008.12.015].

Pierrot, D., E. Lewis, and D. W. R. Wallace. 2006. MS Excel program developed for CO_2 system calculations. ORNL/CDIAC-105a. Carbon Dioxide Information Analysis Center, Oak Ridge National Laboratory, US Department of Energy, Oak Ridge, TN.

———, and others. 2009. Recommendations for autonomous underway pCO_2 measuring systems and data-reduction routines. Deep Sea Res. II 56:512-522 [doi:10.1016/j.dsr2.2008.12.005].

Rubin, S. I., and H. Ping Wu. 2000. A novel fiber-optic sensor for the long-term, autonomous measurement of pCO_2 in seawater, p. 631-639. OCEANS 2000 MTS/IEEE Conference and Exhibition.

Saderne, V., P. Fietzek, and P. M. J. Herman. 2013. Extreme variations of pCO_2 and pH in a macrophyte meadow of the Baltic Sea in summer: Evidence of the effect of photosynthesis and local upwelling. PLoS ONE 8:e62689 [doi:10.1371/journal.pone.0062689].

Shitashima, K. 2010. Evolution of compact electrochemical in-situ pH-pCO_2 sensor using ISFET-pH electrode, p. 1-4. OCEANS 2010.

Tabacco, M. B., M. Uttamial, M. Mcallister, and D. R. Walt. 1999. An autonomous sensor and telemetry system for low-level pCO2 measurements in seawater. Anal. Chem. 71:1483-1483 [doi:10.1021/ac991580p].

Takahashi, T., J. Olafsson, J. G. Goddard, D. W. Chipman, and S. C. Sutherland. 1993. Seasonal variation of CO_2 and nutrients in the high-latitude surface ocean: a comparative study. Global Biogeochem. Cycles 7:843-878 [doi:10.1029/93GB02263].

———, and others. 2009. Climatological mean and decadal change in surface ocean pCO_2, and net sea-air CO_2 flux over the global oceans. Deep-Sea Res. II 56:554-577 [doi:10.1016/j.dsr2.2008.12.009].

Thomas, H., and B. Schneider. 1999. The seasonal cycle of carbon dioxide in Baltic Sea surface waters. J. Mar. Syst. 22:53-67 [doi:10.1016/S0924-7963(99)00030-5].

Turk, D., V. Malačič, M. D. Degrandpre, and W. R. Mcgillis. 2010. Carbon dioxide variability and air-sea fluxes in the northern Adriatic Sea. J. Geophys. Res. 115:C10043 [doi:10.1029/2009JC006034].

———, J. W. Book, and W. R. Mcgillis. 2013. pCO_2 and CO_2 exchange during high bora winds in the Northern Adriatic. J. Mar. Syst. 117-118:65-71 [doi:10.1016/j.jmarsys.2013.02.010].

Wang, Z. A., W. J. Cai, Y. C. Wang, and B. L. Upchurch. 2003. A long pathlength liquid-core waveguide sensor for real-time pCO_2 measurements at sea. Mar. Chem. 84:73-84 [doi:10.1016/S0304-4203(03)00112-9].

Wang, Z. H., Y. H. Wang, W. J. Cai, and S. Y. Liu. 2002. A long pathlength spectrophotometric pCO_2 sensor using a gas-permeable liquid-core waveguide. Talanta 57:69-80.

Watson, A. J., and others. 2009. Tracking the variable North Atlantic sink for atmospheric CO_2. Science 326:1391-1393 [doi:10.1126/science.1177394].

Whitledge, T. E., S. C. Malloy, C. J. Patton, and C. O. Wirick. 1981. Automated nutrient analysis in seawater. Brookhaven National Lab Report 51398:216.

Willcox, S., and others. 2009. An autonomous mobile platform for underway surface carbon measurements in open-ocean and coastal waters, p. 1-8. OCEANS 2009, MTS/IEEE Biloxi - Marine Technology for Our Future: Global and Local Challenges.

Wolf-Gladrow, D. A., R. E. Zeebe, C. Klaas, A. Kortzinger, and A. G. Dickson. 2007. Total alkalinity: The explicit conservative expression and its application to biogeochemical processes. Mar. Chem. 106:287-300 [doi:10.1016/j.marchem.2007.01.006].

Yates, K. K., C. Dufore, N. Smiley, C. Jackson, and R. B. Halley. 2007. Diurnal variation of oxygen and carbonate system parameters in Tampa Bay and Florida Bay. Mar. Chem. 104:110-124 [doi:10.1016/j.marchem.2006.12.008].

Zeebe, R. E., and D. Wolf-Gladrow. 2001. CO_2. *In* Seawater: Equilibrium, kinetics, isotopes. Elsevier.

Submitted 12 October 2013
Revised 3 February 2014
Accepted 13 March 2014